Volume 28
Number 21
3 June 2026
Pages 12665–13262

PCCP

Physical Chemistry Chemical Physics

rsc.li/pccp

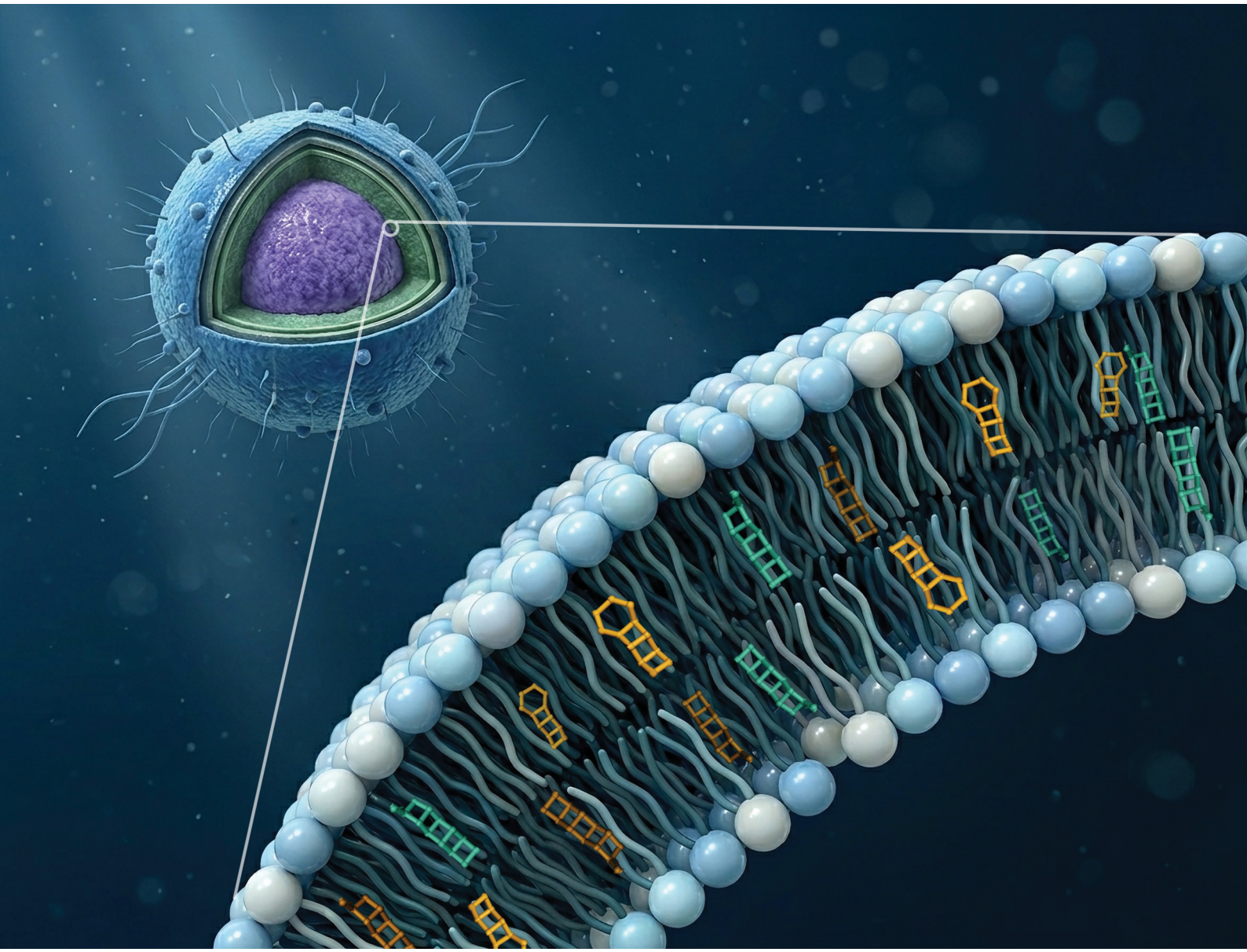

ISSN 1463-9076

ROYAL SOCIETY OF CHEMISTRY

PAPER

František Štěpánek *et al.*

Dense yet flexible: how ladderanes found in anammox bacteria impact phospholipid membrane structure and properties

PCCP Owner Societies

PCCP

ROYAL SOCIETY OF CHEMISTRY

PAPER

View Article Online
View Journal | View Issue

Cite this: *Phys. Chem. Chem. Phys.*, 2026, **28**, 12730

Dense yet flexible: how ladderanes found in anammox bacteria impact phospholipid membrane structure and properties

Terezie Císařová, [a] Martin Balouch, [ab] Jaroslav Hanuš, [a] Karel Berka, [c] Vojtěch Kouba [d] and František Štěpánek *[a]

The composition of phospholipid membranes in cellular organelles is tailored to their functionality and reflects the evolutionary pressures prevailing in specific environmental niches. While many organisms share common membrane motifs, anaerobic ammonium-oxidising bacteria stand out as their membranes are enriched with distinctive ladder-like molecules called ladderanes. Membranes containing these conjugated cyclobutane structures have been studied for their permeation properties, density, and organisation, but their exact biological function remains unclear. In the present work, molecular dynamics simulations were used to investigate the behaviour of phospholipid membranes containing ladderane phospholipids or ladderane alcohols. The simulations showed that increased ladderane phospholipid content disrupted the membrane order and made it more permeable to hydrazine, while ladderane alcohols had a stabilising effect and maintained a well-ordered bilayer structure with low permeability. The results further indicate that compared to common phospholipid membranes, membranes bearing ladderane alcohols possess unusually high fluidity even at low environmental temperatures while retaining a high membrane density comparable to rigid membranes in the gelled state. This phase behaviour of membranes revealed surprising similarities between the roles of ladderane alcohols and cholesterol in terms of membrane fluidity and molecular order, providing a possible new angle on the biological role of these unusual ladder-like molecules in anammox bacteria.

Received 15th January 2026,
Accepted 6th April 2026

DOI: 10.1039/d6cp00146g

rsc.li/pccp

1. Introduction

Anaerobic ammonium-oxidising bacteria, commonly known as anammox bacteria, are organisms discovered in the early 1990s.[1,2] They thrive in diverse environments, including wastewater, freshwater lakes and oceanic regions. Depending on the specific site, these water temperatures can reach below 10 °C or above 30 °C.[3–5] Anammox bacteria host reactions in which ammonium and nitrites are converted mainly to gaseous nitrogen. Interestingly, hydrazine – a highly reactive and toxic compound – plays a role as one of the intermediates during the process.[6] The reactions happen inside the anammoxosome, an organelle bounded by a phospholipid bilayer in which all the crucial anammox enzymes are located. The anammoxosome membrane is characterised by regions with high curvature.[7] The anammoxosome membrane contains molecules with unique motifs. These motifs are called ladderanes as they are composed of conjugated cyclobutanes/cyclohexanes visually resembling a ladder.[8] Two main motifs were observed, the [3]-motif (three conjugated cyclobutanes conjugated with cyclohexane, which is connected to the C-chain) or the [5]-motif (five conjugated cyclobutanes connected to the C-chain). Their structures are shown in Fig. 1. Natural ladderane phospholipids typically contain at least one [3]-motif, molecules containing only [5]-motifs are scarcer.[9,10]

Conjugated cyclobutene rings are uncommon structures in living organisms and generally in nature. The functional role of ladderane motifs in the organelles of bacteria with such an unusual metabolism is still unclear. The hypothesis that ladderane-bearing lipid bilayers could prevent hydrazine from permeating out of the organelle has been undermined by the finding that a membrane composed of ladderane phospholipids exhibits hydrazine permeability comparable to that of a conventional phospholipid bilayer.[11] However, ladderane bilayers exhibit very low proton permeability, suggesting that their role may instead be to preserve the proton motive force.[11,12] It is also

[a] *Department of Chemical Engineering, University of Chemistry and Technology Prague, Technická 5, Prague 6 166 28, Czech Republic. E-mail: stepanef@vscht.cz; Tel: +420 220 443 165*
[b] *Zentiva, K.S., U Kabelovny 130, Prague 10 102 37, Czech Republic*
[c] *Department of Physical Chemistry, Faculty of Science, Palacký University Olomouc, 17. listopadu 12, Olomouc 771 46, Czech Republic*
[d] *Department of Water Technology and Environmental Engineering, University of Chemistry and Technology Prague, Technická 5, 166 28 Prague, Czechia*

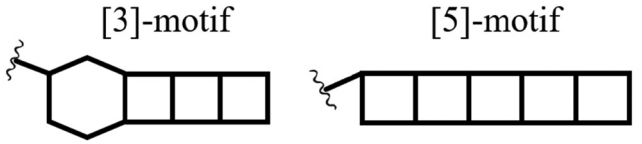

Fig. 1 Natural ladderane motifs, denoted as the [3]-motif (left) and the [5]-motif (right).

possible that ladderane motifs in anammox bacteria have some other, as yet unknown, function.

The properties of lipid bilayers, such as rigidity or permeability for small molecules, are strongly influenced by the membrane phase behavior,[13] which can transition between the sub-gel, flat gel, tilted gel, ripple, and fluid phases.[14] The membrane composition determines a characteristic transition temperature that marks the shift between the gel and the fluid phases.[15] The phase behaviour of membranes can be modulated by the presence of specific molecules such as cholesterol,[16] which can constitute up to 30% of the cellular lipid bilayer in animals,[17] while bacterial membranes typically lack cholesterol. Increasing the cholesterol content condenses the bilayer, reducing the specific area per lipid and the tilt angle of the lipid acyl chains, while increasing bilayer density and thickness.[18] Above the phase transition temperature, cholesterol increases molecular ordering and therefore adds rigidity to the bilayer. Below the phase transition temperature, cholesterol contributes to bilayer fluidization while maintaining a high degree of order.

In living systems, the composition of the bilayer often changes in response to environmental fluctuations, as the membrane must remain within certain limits of fluidity and rigidity required for optimal cell function.[19] In anammox bacteria, membranes are known to contain cholesterol-like bacteriohopanoids such as bacteriohopanetetrol, bacteriohopanetetrol cyclitol ether as well as hopanoid intermediates such as squalene; their highest levels were detected in cold-adapted anammox bacteria,[20] supporting earlier suggestions that these compounds help maintain the balance between membrane fluidity and rigidity.

Exploring the phase behaviour of ladderane membranes could provide valuable insight into natural anammox activity and the role played by ladderane motifs. However, the extraction of pure ladderane molecules from bacterial cultures has proven difficult, and although complete laboratory synthesis of ladderane molecules is in principle possible, the yield has been low.[21] Hence, computational approaches may offer a suitable alternative to physical experiments for exploring ladderane membrane behaviour and provide a powerful tool for *in silico* testing of hypotheses concerning the biological role of ladderane motifs.[22,23]

In this work, computational techniques were employed to explore the influence of ladderane molecules on the phase behaviour and permeability of lipid bilayers. Special emphasis was placed on simulations comparing ladderane lipids and ladderane alcohols, as the experimental analysis of anammox bacteria composition often does not distinguish between the two. The computational approach used in our work was based on the combination of Molecular Dynamics (MD) to resolve the membrane structure at defined temperatures and compositions, and COSMOPerm to evaluate the permeability of small molecules across the membranes. These computational tools nowadays make it possible to simulate bilayers of biologically relevant composition and size[24–26] and evaluate their structure, phase behaviour, electron density profile and other properties of interest with consistent quality.[27–31] The ability to obtain trends for composition-dependent membrane properties from *in silico* models can be used to formulate hypotheses about the possible role of ladderane structures in anammox bacteria.

2. Methodology

2.1. Overall approach and system choice

A series of phospholipid bilayers containing systematically increasing content of ladderane molecules were simulated by molecular dynamics (MD) to examine the influence of ladderane type and concentration on the membrane structure and phase behaviour. Membranes based on two lipids were simulated: DPPC (1,2-dipalmitoylphosphatidylcholine) as a benchmark phospholipid whose phase behaviour is well known in the literature, and IPPC (1-palmitoyl-2-(14-methylpentadecanoyl)-*sn-glycero*-3-phosphocholine) as a representative bacteria-specific phospholipid. Ladderane molecules incorporated into the membranes included two ladderane lipids (LA35 and LA55) and two ladderane alcohols (6OL3 and 6OL5). The rationale behind their choice was the abundance of anammox bacteria and the presence of both [3]- and [5]-motifs. Experimental analysis of anammox bacteria typically provides the total content of ladderane motifs but not their exact source (lipids *vs.* alcohols). Hence, we wanted to compare the effects of ladderane lipids and ladderane alcohols separately – a test that can only be done *in silico* at present. Membranes with cholesterol were simulated as a reference. Cholesterol has been chosen as a reference system not only due to its structural analogy with hopanoids[22] but also because cholesterol-containing membranes represent a well-characterised and extensively studied model in molecular dynamics simulations that serves as a robust benchmark for interpreting membrane behaviour investigated in this work. The structures of all molecules used in the study are shown in Fig. 2. A table of all modelled systems can be found in the SI.

All simulations were performed at 10 °C to mimic the naturally low temperatures that anammox bacteria endure.[3,5] Since IPPC-based membranes are expected to have a lower phase transition temperature than those based on DPPC, thanks to their branching,[32] this temperature choice made it possible to compare the effect of ladderanes on membranes in different phases.

2.2. Molecular dynamics simulations

The input topology files for LA35 and LA55 phospholipids, together with the modified CHARMM36 force field, were generously provided by Himanshu Khandelia and his research group from their previous work.[33] The structural model and force field parameters of IPPC were obtained from the CHARMM-GUI lipid database.[34] The methodology for obtaining topology files for ladderane alcohols, along with the creation of initial bilayer

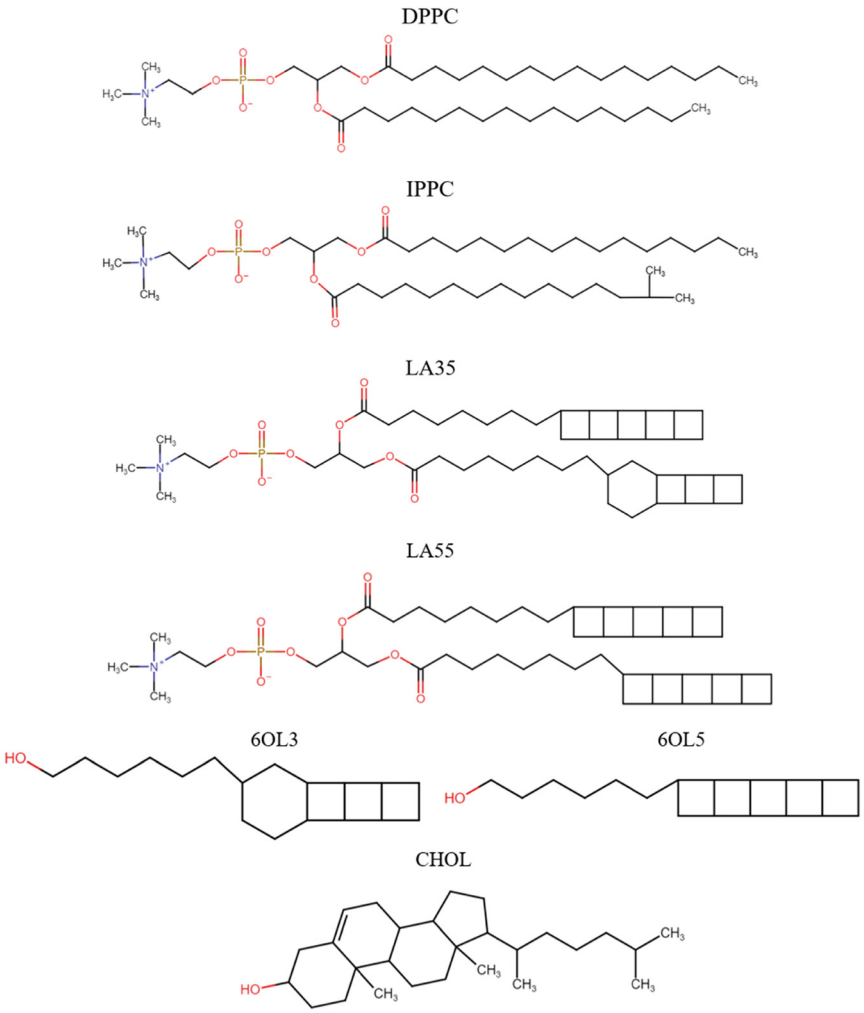

Fig. 2 Structure of molecules used in this work. DPPC (1,2-dipalmitoylphosphatidylcholine) and IPPC (1-palmitoyl-2-(14-methylpentadecanoyl)-*sn*-*glycero*-3-phosphocholine) phospholipids, LA35 (1-(8-[5]-ladderane-octanoyl)-2-(8-[3]-ladderane-octanoyl)-*sn*-*glycero*-1-phosphocholine) and LA55 (1-(8-[5]-ladderane-octanoyl)-2-(8-[5]-ladderane-octanoyl)-*sn*-*glycero*-1-phosphocholine) ladderane lipids, 6OL5 (6-[5]-ladderane-1-hexanol) and 6OL3 (6-[3]-ladderane-1-hexanol) ladderane alcohols, and cholesterol ((3β)-cholest-5-en-3-ol).

conformations of smaller bilayers (128 molecules), is described in detail in the SI. Initial bilayer conformations for larger bilayers (512 molecules) were constructed using the Packmol software.[35] The bilayer systems were then hydrated with TIP3P water, achieving an approximate hydration level of 52 water molecules per lipid.

All molecular dynamics (MD) simulations and some parameter evaluations were performed using GROMACS software, versions 2022 or 2020.1.[36] Energy minimisation was performed using the conjugate gradient algorithm with an initial step size of 0.001 nm and a maximum force threshold of 1000.0 kJ mol^{-1} nm^{-1}. MD simulations were carried out in the constant number, constant temperature, and constant pressure (NpT) ensemble. A leapfrog integrator was employed under three-dimensional periodic boundary conditions with the modified[33] all-atom CHARMM36m force field.[37] The pressure was regulated using the Parrinello–Rahman barostat[38] with semi-isotropic coupling, a reference pressure of 1 bar, a relaxation time of 5 ps, and a compressibility of 4.5×10^{-5} bar^{-1}, consistent with the experimental compressibility of liquid water.

Equilibration runs were performed with a duration of 2 ns each, using a time step of 1 or 2 fs. The temperature was constant in all simulations and maintained at 283 K (10 °C) using a V-rescale thermostat[39] with a coupling constant of 1 ps. Consequently, phase assignments discussed in this work are based on structural and dynamical bilayer descriptors (ordering, thickness, and lateral organisation) at this fixed temperature, rather than on explicitly determined temperature-dependent phase transitions. During NpT (constant number of atoms, constant pressure and temperature) equilibration, the bilayer was expected to rapidly shrink from its high-energy state due to large initial intermolecular distances. After equilibration, simulations were executed with a time step of 2 fs. The temperature was consistently maintained at 283 K (10 °C) using the Nosé–Hoover thermostat,[40] to facilitate the study of ladderane behaviour at lower temperatures. The short-range neighbour list and

electrostatic cutoff distances were set to 1.4 nm, with interactions beyond this range handled by the Particle Mesh Ewald (PME) method. The cutoff distance for short-range van der Waals forces, represented by the Lennard-Jones 12-6 potential, was set to 1.2 nm. The LINCS algorithm[41] was used to constrain all carbon–hydrogen bonds, thus preventing frequent vibrations of light hydrogen atoms. The simulation duration was 300 ns using resources provided by the CESNET Metacentrum. All data evaluations were done from the last 50 ns unless otherwise specified.

2.3. Data analysis and post-processing

Visualisation of the simulated systems was generated using PyMOL software.[42] The bilayer images were taken using the Pymol software as 20 Å wide slices from the region of interest of the bilayer (Fig. S2). The area per lipid parameter was computed by two different approaches. The first approach, non-specific to the molecule, simply used the formula $\mathrm{APL} = \frac{x \cdot y}{N}$, where N is the number of molecules in one leaflet (either 64 or 256) and x, y are the simulation box dimensions. The second approach used the GridMAT-MD software,[43] which finds the specific space of each molecule based on a grid search algorithm. The bilayer thickness was assessed as the average P(phosphorus)–P distance across the bilayer using the same GridMAT-MD software. The density profiles were acquired using the integrated GROMACS function gmx_density.

2.4. Permeability and partitioning coefficient calculation

Permeability is a proportionality coefficient that relates the molar flux, J (mol m^{-2} s^{-1}), of a substance across a bilayer to its concentration driving force, Δc (mol m^{-3}), according to $J = P_{\mathrm{em}}\Delta c$. Permeability in this work was determined for two molecules, hydrazine and 5-fluorouracil. Hydrazine plays a crucial role in the metabolism of anammox bacteria, and its permeability through ladderane-containing membranes has direct relevance for deciphering the possible biological role of conjugated cyclobutane structures in these bacteria. On the other hand, 5-fluorouracil was chosen as a reference as its permeation through conventional phospholipid bilayers has been recently explored in the context of liposomal drug delivery.[44] The membrane/water equilibrium partitioning coefficient is a measure of the tendency of a given molecule to stay in the membrane rather than in an aqueous environment. It is similar, but not identical to the octanol/water partitioning coefficient, which is commonly used as a measure of the lipophilic character of pharmaceutical substances.

Both permeability and the partitioning coefficient were calculated using the COSMOPerm approach.[45] Briefly, representative frames were selected from the equilibrated portion of the trajectory (typically, the last 5 ns of MD simulations were sampled at 0.5 ns to collect the frames). All molecules constituting the membrane were then optimised for both structure and energy. Conformers were generated from SMILES strings using the RDKit package within the KNIME[46] workflow, with up to 20 conformers produced per molecule. All generated conformers were optimised using the default force field MMFF94,[47] and the lowest-energy structures without internal cyclisation were retained. Hydrogen atoms were subsequently added to the selected conformers. Each conformer was further optimised using TURBOMOLE 6.3[48] using DFT/B-P/cc-TZVP vacuum and COSMO water optimisation with a fine grid option. COSMO files were obtained for all conformers, and the conformer with the lowest energy, which is not caused by

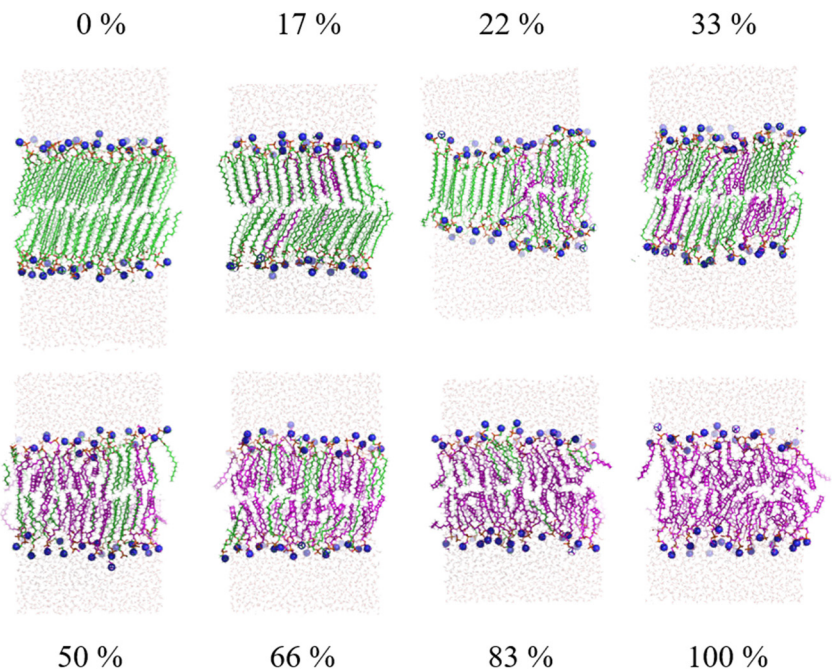

Fig. 3 Visualisation of DPPC-LA35 bilayers, represented by a 20 Å wide cross-sectional slice taken from the final state of the MD simulation. The values indicate the molar percentage of LA35 in the bilayer. The carbons of DPPC molecules are shown in green, carbons of LA35 molecules in magenta, and nitrogen atoms in blue.

internal cyclisation of the ladderane chain, was used for further COSMO calculation using COSMOTherm X18.

3. Results and discussion

3.1. Structure and properties of DPPC-LA35 bilayers

To gain an initial understanding of the structure of phospholipid bilayers containing ladderane lipids, eight bilayers, each consisting of 128 phospholipid molecules with a varying ratio of DPPC and LA35, were composed and subjected to MD simulations as described in Section 2.2. Throughout this publication, all reported contents are given in molar percent (mol%). The chosen simulation temperature of 10 °C was well below the main phase transition temperature of DPPC (41.3 °C).[49] Thus, the pure DPPC membrane (0% of LA35) was in the gel phase, which is characterised by a high degree of order (Fig. 3). With increasing content of LA35, the bilayers gradually became more disordered. In bilayers containing 22–50% of the ladderane lipid, ordering appeared mainly in regions enriched by DPPC molecules. For bilayers with even higher LA35 content, these regions diminished, and a membrane containing 100% of LA35 appeared to be fully in the fluid phase (Fig. 3). The exact phase transition temperature of LA35 is not known, but it follows from these MD simulations that it must be below 10 °C. For comparison, the main transition temperature of a structurally similar phospholipid [5][3]PC was reported to be 11.8 °C[11]

The bilayer containing 17% of LA35 had a cross-tilted arrangement[50] characterised by a V-shaped configuration in which acyl chains from opposing leaflets do not align in parallel. Interestingly, the partial ordering in a bilayer containing 33% of LA35 was of the tilted type (*i.e.*, same as in pure DPPC), with acyl chains from opposing leaflets aligned parallel to each other. Bilayers with 17% and 22% of LA35 both exhibited some rippled regions, *i.e.* regions with a reduced bilayer thickness caused by a partial penetration of acyl chains from opposing leaflets into each other. A detailed cross-sectional scan of such a region taken from the bilayer containing 22% of LA35 is shown in the SI, Fig. S3. The presence of rippled regions in a DPPC membrane at low temperatures has been previously reported.[51] To verify that the presence of the rippled regions was not a size-dependent effect, MD simulations of membranes containing 17%, 22%, 50%, and 83% LA35 were also performed in a 4 times larger system (512 molecules). The results (shown in the SI, Fig. S4) were consistent with those obtained using the default MD simulation domain size.

Quantitatively, the structure of the membranes can be expressed by the area per lipid (APL) and the membrane thickness. These parameters were evaluated from the MD simulations, and their dependence on the membrane composition is shown in Fig. 4. Lower APL indicates reduced molecular movement and increased bilayer order. The APL was found to increase with LA35 content for both bilayer components, confirming the visual observation that pure DPPC was in the ordered gel phase while the increasing proportion of LA35 enhanced bilayer fluidity. The APL value obtained from the MD simulations at 10 °C was 48.9 ± 0.4 Å^2 for pure DPPC, which is consistent with a published experimental value of 47.2 ± 0.5 Å^2 at 20 °C.[52,53] For pure LA35 (which was in the fluid state at 10 °C), the area per lipid from MD simulations was 62.5 ± 0.7 Å^2, which is comparable with a value of 63.1 Å^2 reported in the literature for a fluid DPPC membrane at 50 °C.[54,55]

The membrane thickness (Fig. 4b) was found to decrease with increasing LA35 content in the membrane, which is consistent with the qualitative observation of the bilayer structures. The disordered LA35 acyl chains allowed the bilayer leaflets to come somewhat closer to each other compared to the well-ordered, stretched acyl chains of pure DPPC. The density profile across the membrane (Fig. 5) also reflects the decreasing molecular order;

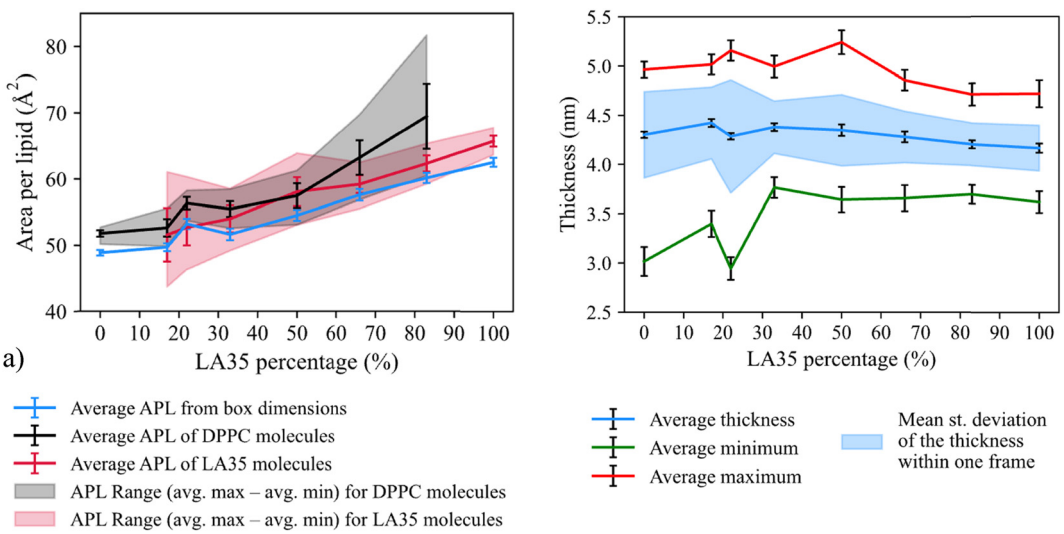

Fig. 4 (a) Area per lipid evaluated from MD simulations for DPPC-LA35 membranes. (b) Membrane thickness as a function of LA35 percentage in the membrane. The error bars represent the standard deviation of the average thickness values of the last 50 ns of the MD simulation, and the blue region signifies the mean standard deviation within one bilayer conformation.

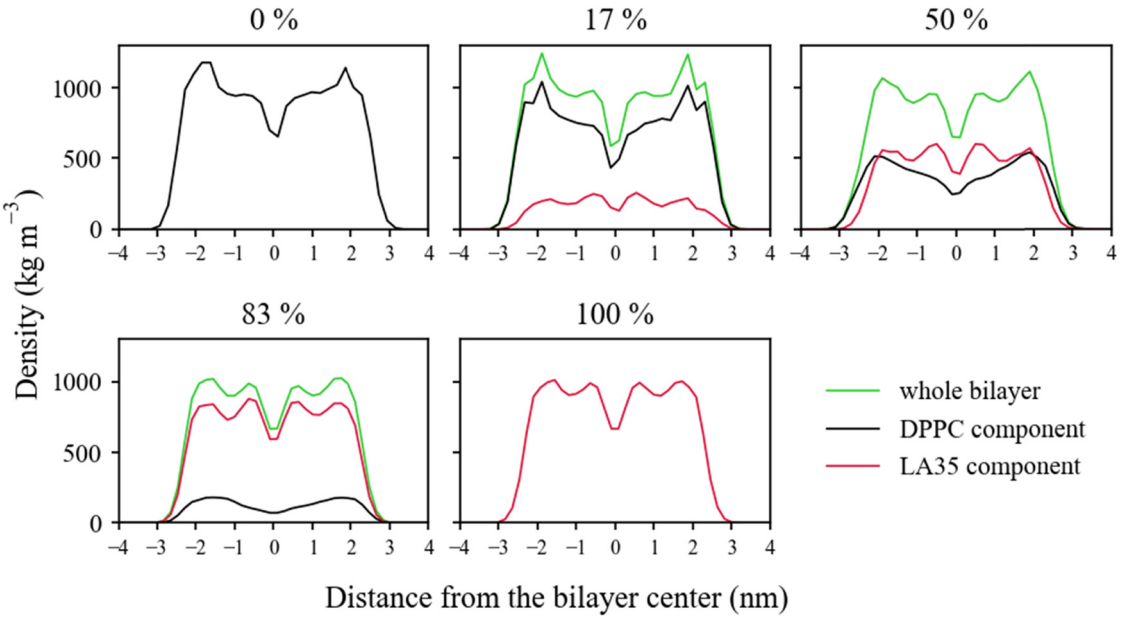

Fig. 5 Density profiles of DPPC-LA35 bilayers with increasing molar percentage of the ladderane lipid as indicated. The density plots are shown for individual components and the whole bilayer. (Density plots including water molecules are shown in the SI, Fig. S10).

Table 1 Calculated permeability ($\log P_{erm}$) and equilibrium bilayer/water partitioning coefficients ($\log K$) of hydrazine and 5-fluorouracil at 10 °C in DPPC-LA35 bilayers of increasing ladderane percentage as indicated

	Hydrazine		5-Fluorouracil	
LA35 in DPPC	$\log P_{erm}$ (cm s^{-1})	$\log K$ (mol mol^{-1})	$\log P_{erm}$ (cm s^{-1})	$\log K$ (mol mol^{-1})
0%	−4.65 ± 0.05	−1.33 ± 0.04	−7.18 ± 0.08	0.41 ± 0.05
17%	−4.55 ± 0.03	−1.18 ± 0.04	−6.67 ± 0.03	0.86 ± 0.05
22%	−4.32 ± 0.06	−1.21 ± 0.03	−6.23 ± 0.02	0.35 ± 0.03
33%	−4.35 ± 0.04	−1.15 ± 0.04	−6.25 ± 0.05	0.42 ± 0.02
50%	−4.14 ± 0.02	−1.09 ± 0.04	−6.02 ± 0.03	0.36 ± 0.04
66%	−4.02 ± 0.09	−1.17 ± 0.08	−5.72 ± 0.19	0.37 ± 0.08
83%	−3.84 ± 0.03	−1.07 ± 0.07	−5.54 ± 0.02	0.16 ± 0.05
100%	−3.92 ± 0.08	−0.72 ± 1.06	−5.50 ± 0.18	0.20 ± 0.14

sharp density maxima corresponding to a tight packing of DPPC molecules gradually disappeared as the percentage of LA35 in the bilayer increased. At higher LA35 contents, a second density maximum in the region of the ladder motif becomes more pronounced, consistent with increasing structural heterogeneity of the membrane. Further discussion of density features and substance integration possibilities is provided in SI, Fig. S9. The decreasing order in DPPC-LA35 bilayers then manifested itself by higher permeability for bilayers with an increasing LA35 content (Table 1). The fact that both permeability and partitioning coefficient of hydrazine increased with increasing LA35 content in the membrane indicates that this ladderane lipid does not appear to improve the resistance of the membrane against hydrazine diffusion.

3.2. Bilayers composed of bacterially derived lipids

While DPPC served as an example of a strongly gelling lipid suitable for testing the effect of ladderanes on the structure and properties of well-ordered bilayers at low temperature, this phospholipid is not natural to anammox bacteria. Therefore, additional MD simulations were performed with bilayers based on IPPC, a structurally similar lipid that contains a branched motif found in anammox membranes (Fig. 2).[56,57] The structures of IPPC-LA35 bilayers with an increasing percentage of the

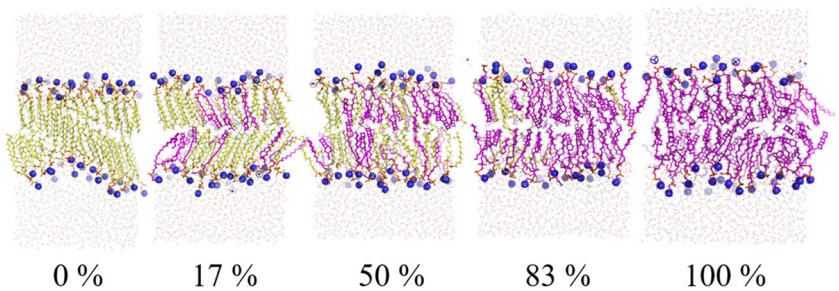

Fig. 6 Visualisation of IPPC-LA35 bilayers, represented by a 20 Å wide cross-sectional slice taken from the final state of the MD simulation. The values indicate the molar percentage of LA35 in the bilayer. The carbons of IPPC molecules are shown in yellow, LA35 carbons in magenta, and nitrogen atoms in blue.

ladderane lipid are shown in Fig. 6. Compared to DPPC-LA35 membranes discussed above, all compositions appeared to be shifted towards less ordered structures. A distinctive rippled phase was observed for a pure IPPC bilayer. With each increment of the LA35 lipid, the bilayer became more fluid.

The area per lipid (APL) of these bilayers follows the same trend as previously observed in DPPC-LA35 bilayers; it gradually increased from around 50 Å^2 for pure IPPC to well over 60 Å^2 for the highly disordered pure LA35 bilayer (Fig. 7a). Interestingly, the average membrane thickness remained almost constant (Fig. 7b), only the pure IPPC bilayer displayed a rather large spread between the minima and the maxima probably due to local presence of the rippled phase. The density profiles (Fig. 8) also followed similar trends as in the case of DPPC-LA35 bilayers, the main difference being the profile of pure IPPC, which did not have the sharp local density maxima that could be seen in pure DPPC membranes. Overall, it can be concluded from these simulations that DPPC is a reasonable choice as a

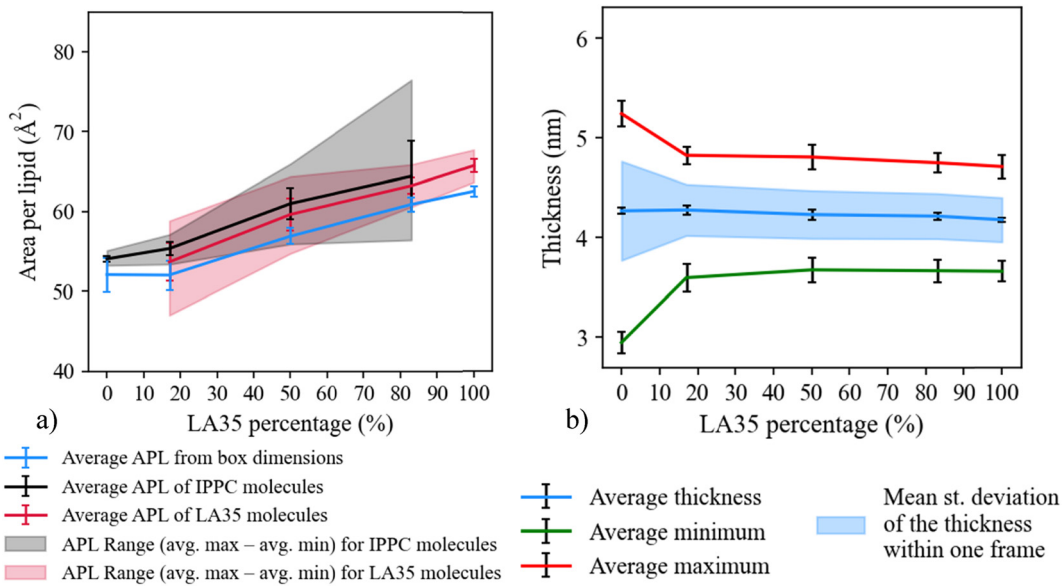

Fig. 7 (a) Area per lipid evaluated from MD simulations for IPPC-LA35 membranes. (b) Membrane thickness as a function of LA35 percentage in the membrane. The error bars represent the standard deviation of the average thickness values of the last 50 ns of the MD simulation, and the blue region signifies the mean standard deviation within one bilayer conformation.

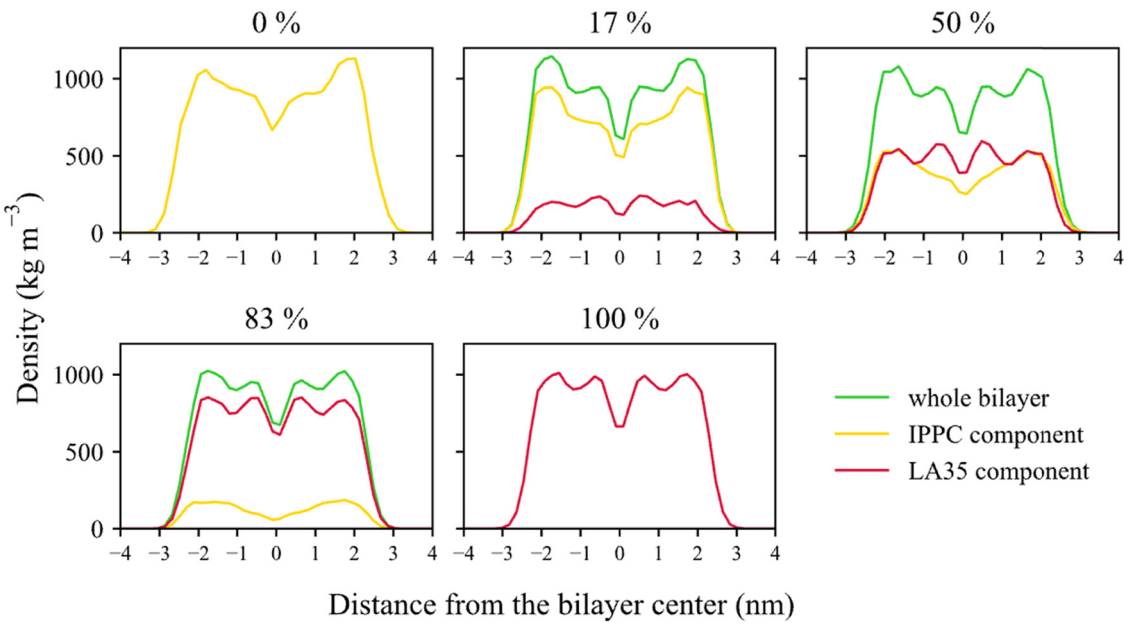

Fig. 8 Density profiles of IPPC-LA35 membranes with increasing molar percentage of the ladderane lipid as indicated. The density plots are shown for individual components and the whole bilayer.

general phospholipid to investigate the effect of ladderanes on the membrane structure.

3.3. Comparison of ladderane lipids and ladderane alcohols with [5] and [3] motifs

Given the diversity of ladderane molecules present in nature,[57,58] further MD simulations were carried out with DPPC bilayers containing an admixture of four different ladderanes (two lipids and two alcohols as detailed in Section 2.1 and shown in Fig. 2) to assess their effect on membrane structure and properties. Cholesterol was included as a reference due to its known stabilising role on phospholipid bilayers. The molar percentage of each investigated substance in the bilayer was fixed at 22% based on the combination of experimentally known composition of anammox organelles and findings from the previous section, where ladderane content around 20% was shown to be sufficient to influence the membrane structure. Note that this percentage is somewhat higher than experimentally reported ladderane alcohol contents found *in vivo*.[56] The resulting membrane structures are shown in Fig. 9.

Visually, bilayers with [5]-motif molecules appeared to be more ordered than those with the [3]-motif. Thus, the addition of LA55 at 22% did not seem to have the same disordering effect as the addition of LA35 investigated in the previous section. All bilayers containing alcohols (both ladderane alcohols and cholesterol) appeared highly ordered, although slight

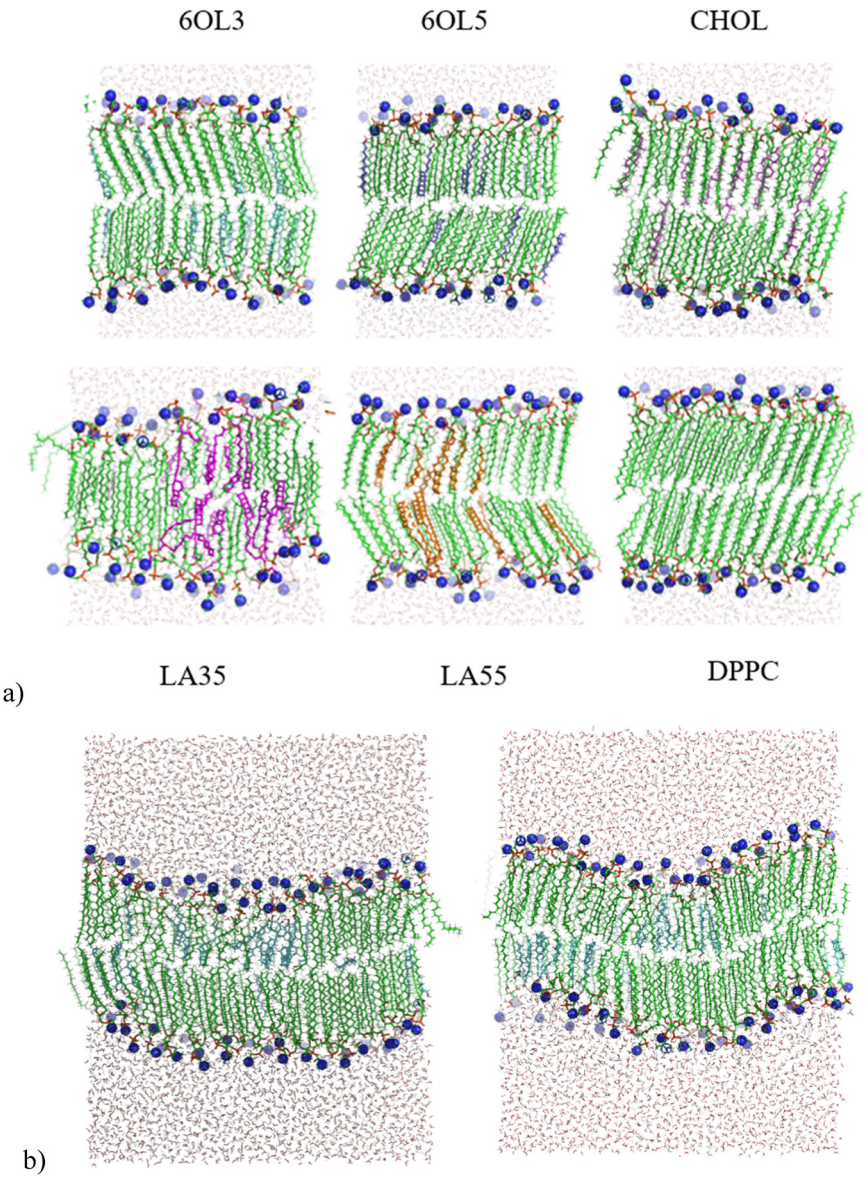

Fig. 9 (a) Visualisation of mixed bilayers, represented by a 20 Å wide cross-sectional slice taken from the final state of the MD simulation. The bilayers consist of DPPC with 22% of a minority component as indicated by the labels. The carbons of DPPC molecules are shown in green, nitrogen atoms in dark blue, and the carbons of minority components by other colours (aquamarine – 6OL3, blue – 6OL5, pink – CHOL, magenta – LA35, orange – LA55). (b) Visualisation of undulations in a DPPC bilayer containing 22% of 6OL3 obtained by MD simulations carried out on a 4 times larger membrane (512 molecules). Two orthogonal slices taken from the same membrane are shown.

variations were observed in the angle of the acyl chains. The 6OL3 composition was also simulated in a 4 times larger bilayer (512 molecules) and the final conformations are shown in Fig. 9b. The high degree of order was preserved but the entire bilayer was noticeably undulated, indicating its elasticity and fluidity. This effect is important, as bilayer fluidity combined with a high degree of order would be essential for a proper biological function of the anammox organelle. The presence of a liquid state in combination with high membrane ordering and undulation at temperatures below the main phase transition is a feature known for bilayers containing cholesterol.[18,59] It was interesting to find that a membrane containing a ladderane alcohol behaves in the same way.

Quantitative descriptors of the membrane structure (area per lipid and membrane thickness) are summarised in Fig. 10. These quantities underline the qualitative observation of the membrane structure. The APL values were notably lower for bilayers containing ladderane alcohols, indicating a high degree of order in these membranes. In fact, the APL values in membranes containing ladderane alcohols (6OL3 and 6OL5) were even lower than in pure DPPC, indicating a densification effect of these molecules that was similar or stronger than that of cholesterol (Fig. 10a). In contrast, both ladderane lipids (LA55 and LA35) increased the area per lipid of DPPC. This suggests that ladderane phospholipid components have a disruptive effect on otherwise well-ordered DPPC bilayers, whereas ladderane alcohols act in the opposite manner. In anammox bacteria, ladderane alcohols might contribute to the condensing effect, enhancing bilayer ordering while maintaining fluidity – a similar role played by cholesterol in the cell membranes of eukaryotes.[60,61]

All bilayers containing alcohols had a slightly higher thickness than those containing ladderane lipids or pure DPPC (Fig. 10b). This difference arose from the more ordered and stretched acyl chains, with the stretching supported by the admixed alcohol molecule chains. Among alcohols, the thickness of 6OL5 and cholesterol bilayers was relatively uniform, while the 6OL3 bilayer exhibited noticeable thickness variability within a single bilayer conformation as indicated by the large spread between the minima and maxima (Fig. 10b). This appears to be a feature of the [3]-motif, as ladderanes containing the [5]-motif (both alcohols and lipids) did not exhibit such thickness variation.

A quantitative insight into the contrasting effect that ladderane lipids and alcohols have on the bilayer structure can be gained from the density plots, shown in Fig. 11. The presence of ladderane lipids (LA35 and LA55) resulted in a decrease in the density of DPPC across the membrane and a reduction of the sharp local density maxima that were originally present in pure DPPC (Fig. 11a). The density pattern of the LA35 and LA55 molecules appeared to have a diffuse character, spanning the entire width of the membrane. In contrast, ladderane alcohols (6OL3 and 6OL5) as well as cholesterol did not alter the DPPC density profile (Fig. 11b). Instead, these molecules appeared to fill local voids (appearing as local density minima) originally present in the pure DPPC membrane, which resulted in the densification of the entire membrane. Compared to the ladderane lipids, ladderane alcohols and cholesterol appeared to be more localised in the membrane. The position of hydroxyl oxygens belonging to the alcohols coincided with the location of DPPC carbonyl and ester oxygens in the bilayer (Fig. 11b). In this way, the alcohol molecules enhanced the density of the bilayer in the region of acyl chains without disrupting the bilayer in the region of the polar heads, enhancing the overall ordering.

The increased density and order of bilayers containing alcohols manifested itself by reduced permeability (Table 2). Compared to the disordering effect observed previously for the LA35 ladderane lipid (Table 1), the permeability of bilayers containing ladderane alcohols was equal to or even lower than

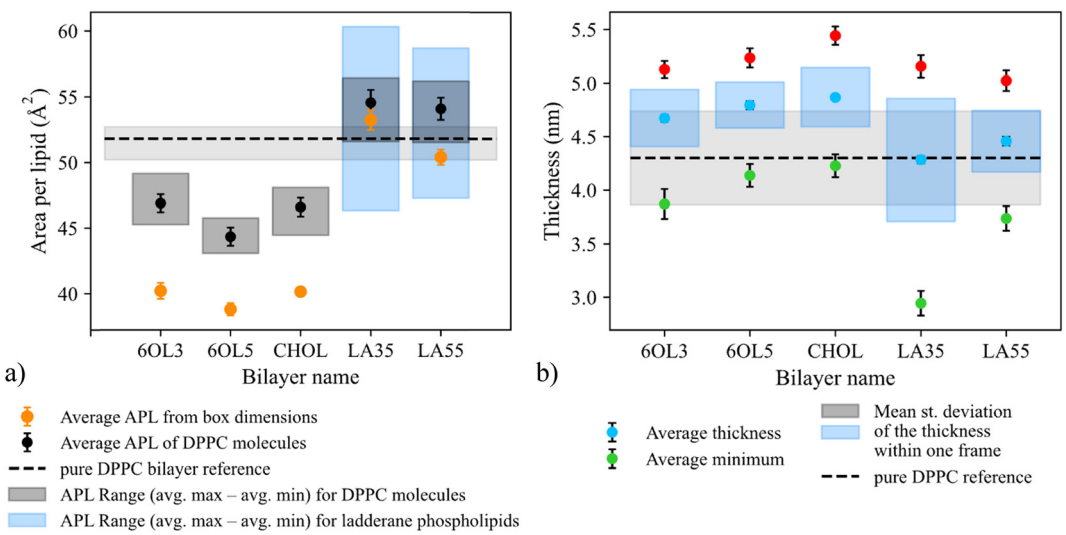

Fig. 10 (a) Area per lipid, and (b) membrane thickness of DPPC membranes containing 22% of ladderanes or cholesterol as indicated. The error bars represent the standard deviation of the average thickness values of the last 50 ns of the MD simulation, and the blue region signifies the mean standard deviation within one bilayer conformation.

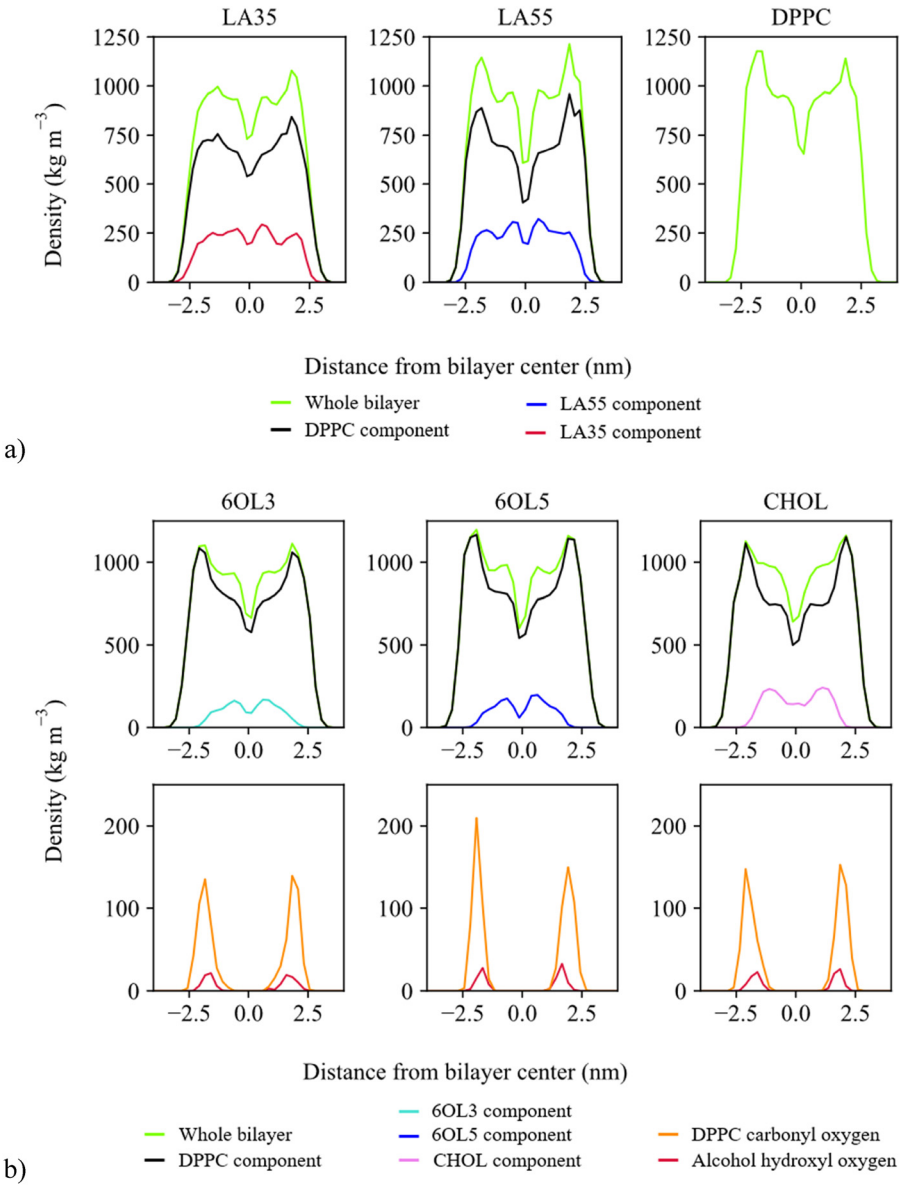

Fig. 11 Density profiles of bilayers containing 22% of ladderane lipids (a) or alcohols (b). The density profiles are plotted for the entire bilayer, individual molecular components of the bilayer, and selected constituent atoms as indicated in the legends.

that of pure DPPC (which is rigid and gelled at 10 °C). The lowest permeability was found for the 6OL5 bilayer, which, however, did not fluidise the bilayer like cholesterol or the 6OL3 molecules.

Table 2 Calculated permeability ($\log P_{erm}$) and equilibrium bilayer/water partitioning coefficients ($\log K$) of hydrazine and 5-fluorouracil at 10 °C in DPPC bilayers containing 22% of ladderane alcohols or cholesterol as indicated. For comparison, values for pure DPPC and a membrane containing 22% of ladderane lipid LA35 are reproduced from Table 1

	Hydrazine		5-Fluorouracil	
	$\log P_{erm}$ (cm s^{-1})	$\log K$ (mol mol^{-1})	$\log P_{erm}$ (cm s^{-1})	$\log K$ (mol mol^{-1})
6OL5	−4.78 ± 0.10	−1.18 ± 0.16	−7.51 ± 0.08	0.55 ± 0.02
6OL3	−4.60 ± 0.10	−1.07 ± 0.10	−7.19 ± 0.11	0.26 ± 0.08
CHOL	−4.64 ± 0.10	−1.41 ± 0.05	−7.36 ± 0.13	0.23 ± 0.04
LA35	−4.32 ± 0.06	−1.21 ± 0.03	−6.23 ± 0.02	0.35 ± 0.03
100% DPPC	−4.65 ± 0.05	−1.33 ± 0.04	−7.18 ± 0.08	0.41 ± 0.05

4. Biological implications

From the results presented above, it appears that the role of ladderane structures in anammox bacteria strongly depends on whether the cyclobutene motifs are present in lipids or alcohols. The main difference in membrane properties attributable to the presence of ladderanes is related to membrane density and fluidity. Maintaining membrane fluidity without sacrificing membrane density even at low temperatures is crucial for high-curvature membrane structures present in some organelles, including anammoxosomes. It has been proposed in the literature that high curvature is a crucial feature for the attachment of

membrane-bound enzymes, which in turn are crucial for specific metabolic pathways such as hydrazine chemistry.[62] Moreover, we hypothesise that the unusual features and local minima of the density profile seen in ladderane-containing membranes could play an additional role in supporting specific enzyme functionality by providing a site for hosting substrates on which the enzymes act. Finally, the similarity of membrane features caused by the presence of ladderane alcohols to those caused by cholesterol lets us hypothesise that evolutionarily distant organisms, such as anammox bacteria and eukaryotes, including higher mammals, have found alternative molecular motifs – along with cholesterol-like bacteriohopanoids – to resolve the same functional objective, namely modifying membrane fluidity and density under specific environmental conditions.

5. Conclusions

The effect of ladderane motifs on the structure and properties of phospholipid bilayers has been investigated using MD simulations. Four different ladderanes – two lipids and two alcohols containing either [3]- or the [5]-motifs – were investigated. At present, *in silico* experiments through MD simulations provide an interesting alternative to physical experiments, as the isolation and purification of ladderane alcohols and lipids separately from natural sources are challenging. Experimental analysis of anammox bacteria homogenates generally provides only information about the overall ladderane content, which makes it difficult to test hypotheses about the possible role of individual structures. Our simulations revealed that the addition of the LA35 ladderane lipid had a disruptive effect on both DPPC and IPPC lipid bilayers, reducing molecular order, increasing the area per lipid and reducing local maxima of membrane density. The membrane disruption caused by the addition of the LA35 lipid increased the membrane permeability for hydrazine, which is a crucial metabolite in anammox bacteria. On the other hand, ladderane alcohols (both 6OL5 and 6OL3) had a densifying effect on DPPC phospholipid bilayers, promoting a highly ordered structure, reducing the area per lipid and increasing the membrane density. Simultaneously, the incorporation of ladderane alcohols supported membrane elasticity without adversely affecting the permeability of hydrazine, which might be crucial for the proper biological function of organelles in anammox bacteria.

Author contributions

Terezie Císařová: methodology, investigation, data curation, visualization, writing – original draft. Martin Balouch: conceptualization, methodology, data curation, writing – original draft. Jaroslav Hanuš: conceptualization, methodology, formal analysis, data curation, visualization, supervision, writing – review & editing. Karel Berka: conceptualization, supervision, resources, writing – review & editing. Vojtěch Kouba: conceptualization, funding acquisition, project administration, writing – review & editing. František Štěpánek: conceptualization, supervision, resources, funding acquisition, writing – review & editing.

Conflicts of interest

The authors declare that they have no known competing financial interests or personal relationships that could have appeared to influence the work reported in this paper.

Data availability

Data for this article are available on Zenodo at DOI: https://doi.org/10.5281/zenodo.18245035.

Supplementary information (SI) contains details of input file creation, verification of domain size dependence, analysis of molecular grouping, and additional density plots. See DOI: https://doi.org/10.1039/d6cp00146g.

Acknowledgements

The authors would like to acknowledge support from the Czech Science Foundation (projects 17–25781S and 24-11986S). F. Š. would like to acknowledge support from the Programme Johannes Amos Comenius under the Ministry of Education, Youth and Sports of the Czech Republic (project no. CZ.02.01.01/00/22_008/0004597). Computational resources were provided by the e-INFRA CZ project (ID:90254), supported by the Ministry of Education, Youth and Sports of the Czech Republic.

References

1 J. G. Kuenen, Anammox Bacteria: From Discovery to Application, *Nat. Rev. Microbiol.*, 2008, **6**(4), 320–326, DOI: 10.1038/nrmicro1857.
2 A. Mulder, A. A. van de Graaf, L. A. Robertson and J. G. Kuenen, Anaerobic Ammonium Oxidation Discovered in a Denitrifying Fluidized Bed Reactor, *FEMS Microbiol. Ecol.*, 1995, **16**(3), 177–183, DOI: 10.1111/j.1574-6941.1995.tb00281.x.
3 Y. Wan, X. Ruan, J. Wang and X. Shi, Spatial and Seasonal Variations in the Abundance of Nitrogen-Transforming Genes and the Microbial Community Structure in Freshwater Lakes with Different Trophic Statuses, *Int. J. Env. Res. Public Health*, 2019, **16**(13), 2298, DOI: 10.3390/ijerph16132298.
4 J. E. Rattray, J. van de Vossenberg, A. Jaeschke, C. E. Hopmans, G. S. Wakeham, G. Lavik, M. M. M. Kuypers, M. Strous, M. S. M. Jetten, S. Schouten and J. S. Sinninghe Damsté, Impact of Temperature on Ladderane Lipid Distribution in Anammox Bacteria, *Appl. Environ. Microbiol.*, 2010, **76**(5), 1596–1603, DOI: 10.1128/AEM.01796-09.
5 W. Wang, W. Liu, D. Wu, X. Wang and G. Zhu, Differentiation of Nitrogen and Microbial Community in the Littoral and Limnetic Sediments of a Large Shallow Eutrophic Lake (Chaohu Lake, China), *J. Soils Sediments*, 2019, **19**(2), 1005–1016, DOI: 10.1007/s11368-018-2090-4.

6 B. Kartal, W. Maalcke and N. M. de Almeida, Molecular Mechanism of Anaerobic Ammonium Oxidation, *Nature*, 2011, **479**(7371), 127–130, DOI: 10.1038/nature10453.
7 L. van Niftrik, W. J. C. Geerts, E. G. van Donselaar, B. M. Humbel, A. Yakushevska, A. J. Verkleij, M. S. M. Jetten and M. Strous, Combined Structural and Chemical Analysis of the Anammoxosome: A Membrane-Bounded Intracytoplasmic Compartment in Anammox Bacteria, *J. Struct. Biol.*, 2008, **161**(3), 401–410, DOI: 10.1016/j.jsb.2007.05.005.
8 D. G. Frickey, The Synthesis and Certain Chemistry of Benzobicyclo(2.2.0)Hexa-2,5-Diene, *Masters thesis*, Kansas State University, 1969. https://hdl.handle.net/2097/26625 (accessed 2024-09-25).
9 J. S. Sinninghe Damsté, M. Strous, W. I. C. Rijpstra, E. C. Hopmans, J. A. J. Geenevasen, A. C. T. van Duin, L. A. van Niftrik and M. S. M. Jetten, Linearly Concatenated Cyclobutane Lipids Form a Dense Bacterial Membrane, *Nature*, 2002, **419**(6908), 708–712, DOI: 10.1038/nature01128.
10 J. E. Rattray, J. van de Vossenberg, E. C. Hopmans, B. Kartal, L. van Niftrik, W. I. C. Rijpstra, M. Strous, M. S. M. Jetten, S. Schouten and J. S. S. Damsté, Ladderane Lipid Distribution in Four Genera of Anammox Bacteria, *Arch. Microbiol.*, 2008, **190**(1), 51–66, DOI: 10.1007/s00203-008-0364-8.
11 F. R. Moss 3rd, S. R. Shuken, J. A. M. Mercer, C. M. Cohen, T. M. Weiss, S. G. Boxer and N. Z. Burns, Ladderane Phospholipids Form a Densely Packed Membrane with Normal Hydrazine and Anomalously Low Proton/Hydroxide Permeability, *Proc. Natl. Acad. Sci. U. S. A.*, 2018, **115**(37), 9098–9103, DOI: 10.1073/pnas.1810706115.
12 S. H. Peeters and L. van Niftrik, Trending Topics and Open Questions in Anaerobic Ammonium Oxidation, *Curr. Opin. Chem. Biol.*, 2019, **49**, 45–52, DOI: 10.1016/j.cbpa.2018.09.022.
13 J. Frallicciardi, J. Melcr, P. Siginou, S. J. Marrink and B. Poolman, Membrane Thickness, Lipid Phase and Sterol Type Are Determining Factors in the Permeability of Membranes to Small Solutes, *Nat. Commun.*, 2022, **13**(1), 1605, DOI: 10.1038/s41467-022-29272-x.
14 M. Kranenburg and B. Smit, Phase Behavior of Model Lipid Bilayers, *J. Phys. Chem. B*, 2005, **109**(14), 6553–6563, DOI: 10.1021/jp0457646.
15 D. G. Ackerman and G. W. Feigenson, Lipid Bilayers: Clusters, Domains and Phases, *Essays Biochem.*, 2015, **46**(57), 33–42, DOI: 10.1042/bse0570033.
16 N. Kučerka, J. Pencer, M.-P. Nieh and J. Katsaras, Influence of Cholesterol on the Bilayer Properties of Monounsaturated Phosphatidylcholine Unilamellar Vesicles, *Eur. Phys. J. E: Soft Matter Biol. Phys.*, 2007, **23**(3), 247–254, DOI: 10.1140/epje/i2007-10202-8.
17 J. Zhang, Q. Li, Y. Wu, D. Wang, L. Xu, Y. Zhang, S. Wang, T. Wang, F. Liu, M. Y. Zaky, S. Hou, S. Liu, K. Zou, H. Lei, L. Zou, Y. Zhang and H. Liu, Cholesterol Content in Cell Membrane Maintains Surface Levels of ErbB2 and Confers a Therapeutic Vulnerability in ErbB2-Positive Breast Cancer, *Cell Commun. Signaling*, 2019, **17**(1), 15, DOI: 10.1186/s12964-019-0328-4.
18 C. T. Boughter, V. Monje-Galvan, W. Im and J. B. Klauda, Influence of Cholesterol on Phospholipid Bilayer Structure and Dynamics, *J. Phys. Chem. B*, 2016, **120**(45), 11761–11772, DOI: 10.1021/acs.jpcb.6b08574.
19 R. N. McElhaney, Effects of Membrane Lipids on Transport and Enzymic Activities. In *Current Topics in Membranes and Transport*, ed Bronner, F., Kleinteller, A., Academic Press, 1982, Vol. 17, pp. 317–380, DOI: 10.1016/S0070-2161(08)60315-9.
20 H. A. Boumann, P. Stroeve, M. L. Longo, B. Poolman, J. M. Kuiper, E. C. Hopmans, M. S. M. Jetten, J. S. Sinninghe Damsté and S. Schouten, Biophysical Properties of Membrane Lipids of Anammox Bacteria: II. Impact of Temperature and Bacteriohopanoids, *Biochim. Biophys. Acta, Biomembr.*, 2009, **1788**(7), 1452–1457, DOI: 10.1016/j.bbamem.2009.04.005.
21 E. N. Hancock and M. K. Brown, Ladderane Natural Products: From the Ground Up, *Chem. – Eur. J.*, 2021, **27**(2), 565–576, DOI: 10.1002/chem.202002866.
22 B. Caron, A. E. Mark and D. Poger, Some Like It Hot: The Effect of Sterols and Hopanoids on Lipid Ordering at High Temperature, *J. Phys. Chem. Lett.*, 2014, **5**(22), 3953–3957, DOI: 10.1021/jz5020778.
23 V. Zhao and J. B. Klauda, Molecular Simulations of Ladderane Lipid Bilayers as Initial Models for Anammox Bacteria, *J. Phys. Chem. B*, 2025, **129**(40), 10325–10332, DOI: 10.1021/acs.jpcb.5c04432.
24 H. J. Risselada and S. J. Marrink, The Molecular Face of Lipid Rafts in Model Membranes, *Proc. Natl. Acad. Sci. U. S. A.*, 2008, **105**(45), 17367–17372, DOI: 10.1073/pnas.0807527105.
25 H. J. Risselada and S. J. Marrink, Curvature Effects on Lipid Packing and Dynamics in Liposomes Revealed by Coarse Grained Molecular Dynamics Simulations, *Phys. Chem. Chem. Phys.*, 2009, **11**(12), 2056–2067, DOI: 10.1039/B818782G.
26 S. J. Marrink, V. Corradi, P. C. T. Souza, H. I. Ingólfsson, D. P. Tieleman and M. S. P. Sansom, Computational Modeling of Realistic Cell Membranes, *Chem. Rev.*, 2019, **119**(9), 6184–6226, DOI: 10.1021/acs.chemrev.8b00460.
27 Å. A. Skjevik, B. D. Madej, C. J. Dickson, C. Lin, K. Teigen, R. C. Walker and I. R. Gould, Simulation of Lipid Bilayer Self-Assembly Using All-Atom Lipid Force Fields, *Phys. Chem. Chem. Phys.*, 2016, **18**(15), 10573–10584, DOI: 10.1039/C5CP07379K.
28 R. Gupta, D. B. Sridhar and B. Rai, Molecular Dynamics Simulation Study of Permeation of Molecules through Skin Lipid Bilayer, *J. Phys. Chem. B*, 2016, **120**(34), 8987–8996, DOI: 10.1021/acs.jpcb.6b05451.
29 A. Ebert and K.-U. Goss, Screening of 6000 Compounds for Uncoupling Activity: A Comparison Between a Mechanistic Biophysical Model and the Structural Alert Profiler Mitotox, *Toxicol. Sci*, 2022, **185**(2), 208–219, DOI: 10.1093/toxsci/kfab139.
30 K. Odehnalová, M. Balouch, K. Storchmannová, E. Petrová, M. Konefał, A. Zadražil, K. Berka, J. Brus and F. Štěpánek, Liposomal Copermeation Assay Reveals Unexpected Membrane Interactions of Commonly Prescribed Drugs, *Mol. Pharmaceutics*, 2024, **21**(6), 2673–2683, DOI: 10.1021/acs.molpharmaceut.3c00766.
31 C. C. Bannan, K. H. Burley, M. Chiu, M. R. Shirts, M. K. Gilson and D. L. Mobley, Blind Prediction of Cyclohexane–Water Distribution Coefficients from the SAMPL5 Challenge,

J. Comput. Aided Mol. Des., 2016, **30**(11), 927–944, DOI: 10.1007/s10822-016-9954-8.

32 D. Poger, B. Caron and A. E. Mark, Effect of Methyl-Branched Fatty Acids on the Structure of Lipid Bilayers, *J. Phys. Chem. B*, 2014, **118**(48), 13838–13848, DOI: 10.1021/jp503910r.

33 V. V. Chaban, M. B. Nielsen, W. Kopec and H. Khandelia, Insights into the Role of Cyclic Ladderane Lipids in Bacteria from Computer Simulations, *Chem. Phys. Lipids*, 2014, **181**, 76–82, DOI: 10.1016/j.chemphyslip.2014.04.002.

34 S. Jo; T. Kim and W. Im, CHARMM-GUI archive – individual lipid molecule library, https://charmm-gui.org/?doc=archive&lib=ipid (accessed 2025-06-29).

35 L. Martínez, R. Andrade, E. G. Birgin and J. M. Martínez, PACKMOL: A Package for Building Initial Configurations for Molecular Dynamics Simulations, *J. Comput. Chem.*, 2009, **30**(13), 2157–2164, DOI: 10.1002/jcc.21224.

36 M. J. Abraham, T. Murtola, R. Schulz, S. Páll, J. C. Smith, B. Hess and E. Lindahl, GROMACS: High Performance Molecular Simulations through Multi-Level Parallelism from Laptops to Supercomputers, *SoftwareX*, 2015, **1–2**, 19–25, DOI: 10.1016/j.softx.2015.06.001.

37 J. Huang, S. Rauscher, G. Nawrocki, T. Ran, M. Feig, B. L. de Groot, H. Grubmüller and A. D. MacKerell, CHARMM36m: An Improved Force Field for Folded and Intrinsically Disordered Proteins, *Nat. Methods*, 2017, **14**(1), 71–73, DOI: 10.1038/nmeth.4067.

38 M. Parrinello and A. Rahman, Polymorphic Transitions in Single Crystals: A New Molecular Dynamics Method, *J. Appl. Phys.*, 1981, **52**(12), 7182–7190, DOI: 10.1063/1.328693.

39 G. Bussi, D. Donadio and M. Parrinello, Canonical Sampling through Velocity Rescaling, *J. Chem. Phys.*, 2007, **126**(1), 014101, DOI: 10.1063/1.2408420.

40 W. G. Hoover and B. L. Holian, Kinetic Moments Method for the Canonical Ensemble Distribution, *Phys. Lett. A*, 1996, **211**(5), 253–257, DOI: 10.1016/0375-9601(95)00973-6.

41 B. Hess, H. Bekker, H. J. C. Berendsen and J. G. E. M. Fraaije, LINCS: A Linear Constraint Solver for Molecular Simulations, *J. Comput. Chem.*, 1997, **18**(12), 1463–1472, DOI: 10.1002/(SICI)1096-987X(199709)18:12%3C1463::AID-JCC4%3E3.0.CO;2-H.

42 L. Schrödinger and W. DeLano, *PyMOL*, 2024. https://www.pymol.org/pymol.

43 W. J. Allen, J. A. Lemkul and D. R. Bevan, GridMAT-MD: A Grid-Based Membrane Analysis Tool for Use with Molecular Dynamics, *J. Comput. Chem.*, 2009, **30**(12), 1952–1958, DOI: 10.1002/jcc.21172.

44 B. Ewert de Oliveira, O. H. Junqueira Amorim, L. L. Lima, R. A. Rezende, N. C. Mestnik, E. Bagatin and G. R. Leonardi, 5-Fluorouracil, Innovative Drug Delivery Systems to Enhance Bioavailability for Topical Use, *J. Drug Delivery Sci. Technol.*, 2021, **61**, 102155, DOI: 10.1016/j.jddst.2020.102155.

45 J. A. H. Schwöbel, A. Ebert, K. Bittermann, U. Huniar, K.-U. Goss and A. Klamt, COSMOperm: Mechanistic Prediction of Passive Membrane Permeability for Neutral Compounds and Ions and Its pH Dependence, *J. Phys. Chem. B*, 2020, **124**(16), 3343–3354, DOI: 10.1021/acs.jpcb.9b11728.

46 M. R. Berthold; N. Cebron; F. Dill; T. R. Gabriel; T. Kötter; T. Meinl; P. Ohl; K. Thiel and B. Wiswedel, *KNIME - the Konstanz Information Miner: Version 2.0 and Beyond. SIGKDD Explor Newsl*, 2009, **11** (1), 26–31, DOI: 10.1145/1656274.1656280.

47 T. A. Halgren, Merck Molecular Force Field. I. Basis, Form, Scope, Parameterization, and Performance of MMFF94, *J. Comput. Chem.*, 1996, **17**(5–6), 490–519, DOI: 10.1002/(SICI)1096-987X(199604)17:5/6%3C490::AID-JCC1%3E3.0.CO;2-P.

48 S. G. Balasubramani, G. P. Chen, S. Coriani, M. Diedenhofen, M. S. Frank, Y. J. Franzke, F. Furche, R. Grotjahn, M. E. Harding, C. Hättig, A. Hellweg, B. Helmich-Paris, C. Holzer, U. Huniar, M. Kaupp, A. Marefat Khah, S. Karbalaei Khani, T. Müller, F. Mack, B. D. Nguyen, S. M. Parker, E. Perlt, D. Rappoport, K. Reiter, S. Roy, M. Rückert, G. Schmitz, M. Sierka, E. Tapavicza, D. P. Tew, C. van Wüllen, V. K. Voora, F. Weigend, A. Wodyński and J. M. Yu, TURBOMOLE: Modular Program Suite for Ab Initio Quantum-Chemical and Condensed-Matter Simulations, *J. Chem. Phys.*, 2020, **152**(18), 184107, DOI: 10.1063/5.0004635.

49 R. L. Biltonen and D. Lichtenberg, The Use of Differential Scanning Calorimetry as a Tool to Characterize Liposome Preparations, *Chem. Phys. Lipids*, 1993, **64**(1), 129–142, DOI: 10.1016/0009-3084(93)90062-8.

50 S. Leekumjorn and A. K. Sum, Molecular Studies of the Gel to Liquid-Crystalline Phase Transition for Fully Hydrated DPPC and DPPE Bilayers, *Biochim. Biophys. Acta, Biomembr.*, 2007, **1768**(2), 354–365, DOI: 10.1016/j.bbamem.2006.11.003.

51 P. Khakbaz and J. B. Klauda, Investigation of Phase Transitions of Saturated Phosphocholine Lipid Bilayers via Molecular Dynamics Simulations, *Biochim. Biophys. Acta, Biomembr.*, 2018, **1860**(8), 1489–1501, DOI: 10.1016/j.bbamem.2018.04.014.

52 S. Tristram-Nagle, R. Zhang, R. M. Suter, C. R. Worthington, W. J. Sun and J. F. Nagle, Measurement of Chain Tilt Angle in Fully Hydrated Bilayers of Gel Phase Lecithins, *Biophys. J.*, 1993, **64**(4), 1097–1109, DOI: 10.1016/S0006-3495(93)81475-9.

53 J. F. Nagle, P. Cognet, F. G. Dupuy and S. Tristram-Nagle, Structure of Gel Phase DPPC Determined by X-Ray Diffraction, *Chem. Phys. Lipids*, 2019, **218**, 168–177, DOI: 10.1016/j.chemphyslip.2018.12.011.

54 H. I. Petrache, S. W. Dodd and M. F. Brown, Area per Lipid and Acyl Length Distributions in Fluid Phosphatidylcholines Determined by 2H NMR Spectroscopy, *Biophys. J.*, 2000, **79**(6), 3172–3192, DOI: 10.1016/S0006-3495(00)76551-9.

55 N. Kučerka, M.-P. Nieh and J. Katsaras, Fluid Phase Lipid Areas and Bilayer Thicknesses of Commonly Used Phosphatidylcholines as a Function of Temperature, *Biochim. Biophys. Acta, Biomembr.*, 2011, **1808**(11), 2761–2771, DOI: 10.1016/j.bbamem.2011.07.022.

56 J. S. Sinninghe Damsté, W. I. C. Rijpstra, J. A. J. Geenevasen, M. Strous and M. S. M. Jetten, Structural Identification of Ladderane and Other Membrane Lipids of Planctomycetes Capable of Anaerobic Ammonium Oxidation (Anammox, *FEBS J.*, 2005, **272**(16), 4270–4283, DOI: 10.1111/j.1742-4658.2005.04842.x.

57 V. Kouba, K. Hůrková, K. Navrátilová, D. Kok, A. Benáková, M. Laureni, P. Vodičková, T. Podzimek, P. Lipovová, L. van

Niftrik, J. Hajšlová, M. C. M. van Loosdrecht, D. G. Weissbrodt and J. Bartáček, Effect of Temperature on the Compositions of Ladderane Lipids in Globally Surveyed Anammox Populations, *Sci. Total Environ.*, 2022, **830**, 154715, DOI: 10.1016/j.scitotenv.2022.154715.

58 V. Kouba, K. Hůrková, K. Navrátilová, D. Kok, A. Benáková, M. Laureni, P. Vodičková, T. Podzimek, P. Lipovová, L. van Niftrik, J. Hajšlová, M. C. M. van Loosdrecht, D. G. Weissbrodt and J. Bartáček, On Anammox Activity at Low Temperature: Effect of Ladderane Composition and Process Conditions, *Chem. Eng. J. Amst. Neth.*, 2022, **445**, 136712, DOI: 10.1016/j.cej.2022.136712.

59 P. F. Almeida, A Simple Thermodynamic Model of the Liquid-Ordered State and the Interactions between Phospholipids and Cholesterol, *Biophys. J.*, 2011, **100**(2), 420–429, DOI: 10.1016/j.bpj.2010.12.3694.

60 W. K. Subczynski, M. Pasenkiewicz-Gierula, J. Widomska, L. Mainali and M. Raguz, High Cholesterol/Low Cholesterol: Effects in Biological Membranes: A Review, *Cell Biochem. Biophys.*, 2017, **75**(3), 369–385, DOI: 10.1007/s12013-017-0792-7.

61 O. G. Mouritsen and M. J. Zuckermann, What's so Special about Cholesterol, *Lipids*, 2004, **39**(11), 1101–1113, DOI: 10.1007/s11745-004-1336-x.

62 Y.-T. Xiong, X.-W. Liao, J.-S. Guo, F. Fang, Y.-P. Chen and P. Yan, Potential Role of the Anammoxosome in the Adaptation of Anammox Bacteria to Salinity Stress, *Environ. Sci. Technol.*, 2024, **58**(15), 6670–6681, DOI: 10.1021/acs.est.4c01417.